

Discovery of 4-Aryl-*N*-arylcarbonyl-2-aminothiazoles as Hec1/Nek2 Inhibitors. Part I: Optimization of in Vitro Potencies and Pharmacokinetic Properties

Ying-Shuan E. Lee,[†] Shih-Hsien Chuang,[†] Lynn Y. L. Huang,[‡] Chun-Liang Lai,[†] Yu-Hsiang Lin,[†] Ju-Ying Yang,[†] Chia-Wei Liu,[†] Sheng-chuan Yang,[†] Her-Sheng Lin,[†] Chia-chi Chang,[‡] Jun-Yu Lai,[§] Pei-Shiou Jian,[§] King Lam,[†] Jia-Ming Chang,[†] Johnson Y. N. Lau,[‡] and Jiann-Jyh Huang^{*,†,§}

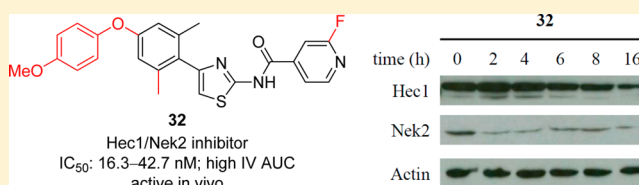
[†]Development Center for Biotechnology, No. 101, Lane 169, Kangning Street, Xizhi District, New Taipei City 22180, Taiwan

[‡]Taivex Therapeutics Corporation, 17th Floor, No. 3, Yuanqu Street, Nangang District, Taipei City 115, Taiwan

[§]Department of Applied Chemistry, National Chiayi University, No. 300, Syuefu Road, Chiayi City 60004, Taiwan

S Supporting Information

ABSTRACT: A series of 4-aryl-*N*-arylcarbonyl-2-aminothiazoles of scaffold 4 was designed and synthesized as Hec1/Nek2 inhibitors. Structural optimization of 4 led to compound 32 bearing C-4' 4-methoxyphenoxy and 4-(*o*-fluoropyridyl)-carbonyl groups that showed low nanomolar in vitro antiproliferative activity (IC₅₀: 16.3–42.7 nM), high intravenous AUC (64.9 μM·h, 2.0 mg/kg) in SD rats, and significant in vivo antitumor activity (T/C = 32%, 20 mg/kg, IV) in mice bearing human MDA-MB-231 xenografts. Cell responses resulting from Hec1/Nek2 inhibition were observed in cells treated with 32, including a reduced level of Hec1 coimmunoprecipitated with Nek2, degradation of Nek2, mitotic abnormalities, and apoptosis. Compound 32 showed selectivity toward cancer cells over normal phenotype cells and was inactive in a [³H]astemizole competitive binding assay for hERG liability screening. Therefore, 32 is as a good lead toward the discovery of a preclinical candidate targeting Hec1/Nek2 interaction.



in mice bearing human MDA-MB-231 xenografts. Cell responses resulting from Hec1/Nek2 inhibition were observed in cells treated with 32, including a reduced level of Hec1 coimmunoprecipitated with Nek2, degradation of Nek2, mitotic abnormalities, and apoptosis. Compound 32 showed selectivity toward cancer cells over normal phenotype cells and was inactive in a [³H]astemizole competitive binding assay for hERG liability screening. Therefore, 32 is as a good lead toward the discovery of a preclinical candidate targeting Hec1/Nek2 interaction.

INTRODUCTION

Highly expressed in cancer 1 (Hec1) is a key component of the kinetochore that regulates the spindle check point and plays an essential role in mitosis.¹ With Nuf2, Spc24, and Spc25, it forms a dumbbell-like heterotetramer called the Ndc80 complex, in which Hec1 and Nuf2 dimerize as a subcomplex, with their globular domains heading toward the microtubule-binding interface.^{2–4} Hec1 has microtubule-binding activity at its N-terminal region (aa 1–196) and is responsible for proper kinetochore–microtubule attachment.^{2,5,6}

Hec1 possesses oncogenic properties: its hyperactivation in transgenic mice leads to tumor formation.⁷ Overexpression of Hec1 is found in various cancers⁸ and correlates with poor prognosis for cancer patients.^{9,10} RNA interference of Hec1 enhances the sensitivity of human ovarian cancer cells to paclitaxel¹¹ and reduces the size of induced adenocarcinomas in nude mice.¹² Because phosphorylation of Hec1 by Nek2 kinase is essential for its mitotic function,^{13–15} disruption of Hec1/Nek2 protein–protein interaction by small molecules shows anticancer activities^{16,17} and may have potential for cancer treatment.

4-Aryl-*N*-phenylcarbonyl-2-aminothiazole 1 (INH1, Figure 1) is the prototype Hec1 inhibitor discovered from a chemical genetic screening.¹⁷ It specifically disrupts Hec1/Nek2 interaction via direct Hec1 binding and shows in vitro

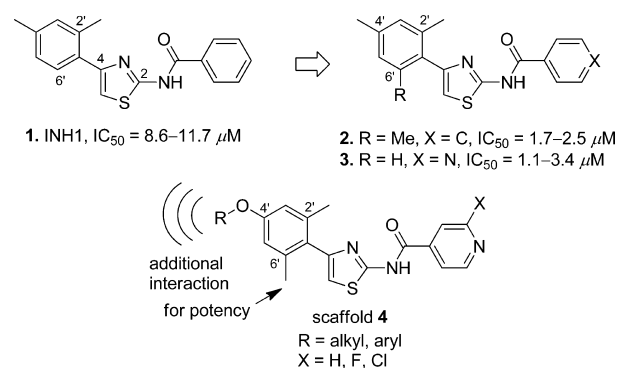


Figure 1. Structures of 4-aryl-*N*-arylcarbonyl-2-aminothiazoles 1–3 and scaffold 4.

antiproliferative activity (IC₅₀: 8.6–11.7 μM) as well as in vivo antitumor activity in MDA-MB-468 xenografts. Subsequent lead optimizations of the *N*-phenylcarbonyl moiety and C-6' position of 1 afforded compounds 2 and 3 that demonstrated improved in vitro potency (IC₅₀: 1.1–3.4 μM).¹⁶ Compounds 1–3 trigger the cellular responses resulting from Hec1 inhibition, including the reduction of Nek2 protein

Received: December 28, 2013

Published: April 28, 2014

level and mitotic abnormalities.^{16,17} Although they are the only reported Hec1/Nek2 inhibitors to date, none of them, 1–3, have been moved into clinical trials.

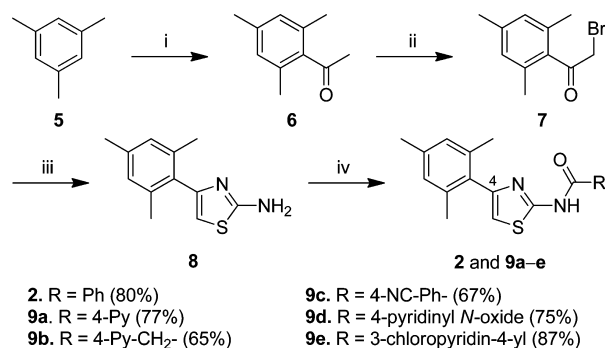
When the structure–activity relationship of 1–3, shown in Figure 1, was examined, compound 2, bearing C-2' and C-6' dimethyls, was found to be ~5-fold more potent than compound 1, bearing a sole C-2' methyl (IC_{50} : 1.7–2.5 μM for 2 and 8.6–11.7 μM for 1). Compound 3, with a 4-pyridylcarbonyl group, also showed ~5-fold improved potency (IC_{50} : 1.1–3.4 μM) compared to 1, which has a phenylcarbonyl group at the same position. As for the C-4' position, no substituent other than a methyl group has been reported on 1–3 and their analogues in the literature.¹⁶ This information suggested that the scaffold of 1–3 possessing C-2' and C-6' dimethyl and 4-pyridylcarbonyl groups could show improved potency and that further structural optimization could be performed on the less explored C-4' position.

Herein, we report the design and synthesis of 4-aryl-*N*-arylcarbonyl-2-aminothiazoles of scaffold 4 as Hec1 inhibitors (Figure 1). Scaffold 4 possesses 2',6'-dimethyl and 4-pyridylcarbonyl groups as the core, various C-4' alkoxy or aryloxy groups, and *o*-halo at the pyridyl group for optimization. After evaluation, we obtained compound 32 with low nanomolar in vitro IC_{50} values, good pharmacokinetic properties, and significant in vivo antitumor activity. Compound 32 induced cellular responses resulting from Hec1 inhibition and was less active on normal cells, kinases, and hERG. In our attempt to discover a preclinical candidate that disrupts Hec1/Nek2 interaction, compound 32 serves as a good lead for future development.

CHEMISTRY

Scheme 1 presents the synthesis of 4-mesityl-*N*-acyl-2-aminothiazoles 2 and 9a–e to verify the design of scaffold 4.

Scheme 1. Synthesis of 4-Mesityl-*N*-acyl-2-aminothiazoles 2 and 9a–e^a



^aReagents and conditions: (i) BiCl₃, acetyl chloride, 70 °C, 83%; (ii) CuBr₂, EtOAc, reflux, 95%; (iii) thiourea, EtOH, reflux, 90%; (iv) RCOCl, DMAP, CH₂Cl₂, 65–87%.

Mesitylene (5) was acylated with acetyl chloride using BiCl₃ as the catalyst to provide acetyl mesitylene 6 in 83% yield.¹⁸ Compound 6 was monobrominated at the α carbon of the acetyl group by CuBr₂ in EtOAc to afford compound 7 in 95% yield. After reacting with thiourea, 7 was converted to 4-mesityl-2-aminothiazole 8 in 90% yield. Acylation of 8 with various acyl chlorides gave corresponding compounds 2 and 9a–e in 65–87% yields.

For the synthesis of 4-aryl-*N*-arylcarbonyl-2-aminothiazoles of scaffold 4 bearing various C-4' alkoxy substituents (R = alkyl in 4, Figure 1), acetophenones 10a–f were brominated by TBABr₃ in CH₃CN and then reacted with thiourea in EtOH to provide corresponding 4-aryl-2-aminothiazoles 11a–f in 57–82% yields (Scheme 2). Acylation of 11a–f with isonicotinoyl chloride, 2-fluoroisonicotinoyl chloride, or 2-chloroisonicotinoyl chloride in CH₂Cl₂ using DMAP as the base afforded desired 4-aryl-*N*-arylcarbonyl-2-aminothiazoles 12–20 possessing various C-4' alkoxy groups in 49–99% yields.

The synthesis of scaffold 4 bearing various C-4' aryloxy substituents (R = aryl in 4, Figure 1) was carried out by the use of 1-(4-amino-2,6-dimethylphenyl)ethanone 21 as the starting material (Scheme 3). The amino group in 21 was transformed into a chloro group by Sandermeyer-type reaction using *t*-BuONO and CuCl₂¹⁹ in CH₃CN to provide 1-(4-chloro-2,6-dimethylphenyl)ethanone 22 in 76% yield. *O*-Arylation of various aryl alcohols by 22 using the Pd(OAc)₂/*t*-BuXPhos catalytic system²⁰ afforded 4-aryloxy-2,6-dimethylacetophenones 23a–i in 19–86% yields. After reacting with TBABr₃ and thiourea, 23a–i were converted to corresponding 4-aryl-2-aminothiazoles 24a–i in 53–96% yields. Acylation of 24a–i with isonicotinoyl chloride or 2-fluoroisonicotinoyl chloride afforded desired 4-aryl-*N*-arylcarbonyl-2-aminothiazoles 25–34 bearing various C-4' aryloxy groups in 17–95% yields.

RESULTS AND DISCUSSION

In Vitro Potency of Scaffold 4. The in vitro potency of the 4-aryl-*N*-arylcarbonyl-2-aminothiazoles of scaffold 4 (Figure 1) was evaluated against the proliferation of HeLa (cervical cancer), K562 (leukemia), MDA-MB-468 (breast cancer), and MDA-MB-231 (breast cancer) cancer cells. Reference compound 2 was tested first. As presented in Table 1, compound 2 showed similar potency (IC_{50} : 2.2–3.6 μM) to that reported in the literature (IC_{50} : 1.7–2.5 μM).¹⁶ Compound 9a, bearing 2',6'-dimethyl and 4-pyridylcarbonyl groups, was 5.4–10.7-fold more potent than 2. The results verified the design of scaffold 4 to improve in vitro potency. We then substituted the 4-pyridylcarbonyl in 9a with various acyl groups to establish the structure–activity relationship. Compound 9b with a methylene elongation to 9a showed similar potency (IC_{50} : 0.30–0.62 μM) to that of 9a. Bioisosteric replacement of the 4-pyridyl in 9a with a 4-cyanophenyl group generated 9c with ~2-fold reduced potency on K562, MDA-MB-468, and MDA-MB-231 cells. Conversion of the pyridyl group in 9a to pyridyl *N*-oxide afforded compound 9d with >4-fold reduced potency (IC_{50} : 2.7 to >10 μM). Introduction of an *o*-chloro group to the 4-pyridyl group in 9a provided compound 9e with slightly reduced potency (IC_{50} : 0.42–0.77 μM).

Considering the structural complexities and possible physicochemical properties of 9a, 9b, and 9e, which possessed similar in vitro potencies, we selected the 4-pyridylcarbonyl group for the following optimization. Turning to the C-4' position of scaffold 4 (Figure 1), we found that the introduction of an alkoxy group showed enhanced antiproliferative activity (Table 2). Compounds 12, 16, 17, 19, and 20, with the corresponding C-4' methoxy, ethoxy, *i*-propoxy, *i*-butoxy, and *c*-pentoxy groups, were more potent than 9a, which possesses a C-4' methyl group, and displayed IC_{50} values ranging from 42.1–392 nM (cf. Table 1, IC_{50} : 300–760 nM for 9a). The increasing size of the C-4' substituents from the methoxy to the *c*-pentoxy groups did not reduce the potency,

Table 1. In Vitro Antiproliferative Activity of *N*-Acyl-4-mesityl-2-aminothiazoles **2** and **9a–e** toward HeLa, K562, MDA-MB-468, and MDA-MB-231 Cancer Cells

2 and 9a–e

compd	R	antiproliferative IC ₅₀ (μM) ^a			
		HeLa	K562	MB468	MB231
2		3.6	3.2	2.2	3.2
9a		0.67	0.43	0.35	0.30
9b		0.62	0.38	0.30	0.31
9c		>10	0.75	0.59	0.61
9d		2.7	9.6	8.7	>10
9e		0.64	0.57	0.77	0.42

^aThe IC₅₀ values were averaged from two independent dose–response curves; variation was generally <15%.

the ortho position of the pyridyl group in **31** generated compound **32** with comparable in vitro antiproliferative activity (IC₅₀: 16.3–42.7 nM). In comparison with lead compound **1**, compound **32** possessed 55–196-fold enhanced potency.

Pharmacokinetics and In Vivo Xenograft. To determine the pharmacokinetic properties of the analogues of scaffold **4**, representative compounds **9a**, **12**, **17**, **31**, and **32** with different substituents at the C-4' position and/or the *o*-fluoro atom to the pyridyl nitrogen were subjected to pharmacokinetic study in Sprague–Dawley rats. The results presented in Table 4 show that prototype **9a**, bearing a C-4' methyl group, possessed an intravenous (IV) AUC value of 5.78 μM·h with good oral bioavailability (41.9%). However, its clearance (CL) was high (23.2 mL/min/kg). Compared to **9a**, compound **12**, possessing a C-4' methoxy group, showed a >5-fold improvement in the AUC (32.7 μM·h) with reduced clearance (3.02 mL/min/kg). Nevertheless, its V_d value was low (0.250 L/kg), and its bioavailability was reduced (20.6%). Compound **17**, with a C-4' *i*-propoxy group, possessed a slightly increased AUC (44.3 μM·h) and V_d (0.769 μM·h) as well as similar clearance and bioavailability compared to that of **12**. Compound **31**, possessing a C-4' 4-methoxyphenoxy group, showed a slightly reduced AUC with increased V_d compared to that of **17**. However, its bioavailability was reduced to 12.4%.

Compound **32**, the fluoro analogue of **31**, possessed the highest IV AUC (64.9 μM·h) among the compounds in Table 4, with a reasonable V_d (0.948 L/kg) and clearance (1.22 mL/min/kg). However, it showed the lowest bioavailability (*F* = 4.6%). This result was not surprising because the *o*-fluoro atom reduced the basicity of the pyridyl nitrogen, thus decreasing the solubility of **32** in acidic gastric fluids, which then retarded its absorption. The solubilities of **9a** and **32** in PBS buffer (pH

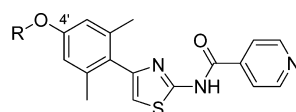
7.4) containing 1% DMSO at 37 °C were 3.33 ± 0.14 and 0.19 ± 0.011 μM, respectively. As a result of this observation, we changed the original 1% methylcellulose formulation to a 5% DMSO, 10% cremophor, and 85% water solution to improve the solubility of **32**. The bioavailability significantly increased to 22.7% (Table 4). The result suggested that solubility might govern the bioavailability of **32**.

To realize an improved PK profile of **32**, we studied the metabolic stability of **9a** and **32** in rat liver microsomes. The half-life (*t*_{1/2}) of **9a** and **32** was found to be 11.0 and 340 min, respectively. As a result, the higher metabolic stability of **32** contributed to its higher AUC (64.9 μM·h) and lower clearance (1.22 mL/min/kg) in comparison with that of **9a** (AUC: 5.78 μM·h and CL: 23.2 mL/min/kg).

Because compound **32** possessed low nanomolar IC₅₀ values (16.3–42.7 nM) with the highest IV and acceptable oral (PO) AUCs, it was selected for in vivo study using nude mice bearing MDA-MB-231 human breast cancer xenografts. As shown in Figure 2, mice treated with 20 mg/kg of **32** for 28 days via daily IV injection showed significant in vivo antitumor activity, with a T/C value of 32% on day 28. Treatment of mice with 150 mg/kg of **32** via oral gavage twice a day also showed antitumor activity, with a T/C value of 57% on day 28, despite being less active as an IV injection. The results reflected the different AUCs between IV and PO routes. Meanwhile, **32** was well-tolerated during the experiments and did not cause significant body weight loss (<5.0%, data not shown) in the test animals. These findings suggested that compound **32** could be a promising anticancer lead because of its good potency and tolerability.

Mechanism of Action. To confirm the mechanism of action of promising lead **32**, we performed a coimmunopre-

Table 2. In Vitro Antiproliferative Activity of 4-Aryl-N-(4-pyridylcarbonyl)-2-aminothiazoles 12, 16, 17, 19, 20, 25–31, 33, and 34 Bearing a C-4' Alkoxy or Aryloxy Group



12, 16, 17, 19, 20, 25–31, 33, and 34

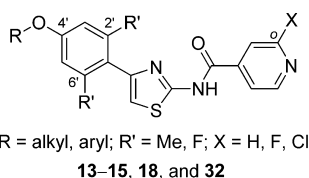
compd	R	antiproliferative IC ₅₀ (nM) ^a			
		HeLa	K562	MB468	MB231
12	Me	99.5	172	150	160
16	Et	42.1	206	170	170
17		162	52.0	120	96.0
19		284	114	392	284
20		215	124	125	96.0
25		236	94.4	150	170
26		237	134	217	136
27		184	172	166	169
28		>1,000	727	>1,000	933
29		260	280	254	239
30		132	58.2	114	106
31		48.6	34.9	37.0	32.0
33		253	102	200	200
34		106	45.7	128	68.0

^aThe IC₅₀ values were averaged from two independent dose–response curves; variation was generally <15%.

precipitation (Co-IP) assay using DMSO- and **32**-treated K562 cells for the immunoprecipitation of Nek2 (Figure 3A). A reduced level of coimmunoprecipitated Hec1 was observed in cells treated with 100 nM **32** (lane 3) relative to cells treated with DMSO (lane 2). In comparison with the literature data of **1**, in which it shows activity in the Co-IP assay at a concentration of 25 μM, the results indicated that the disruption of Hec1/Nek2 protein–protein interaction by **32** took place in the cells with improved potency. To provide more evidence, we analyzed the effect of **32** on the Nek2 protein level in K562 cells by western blotting. Compound **32** led to the degradation of Nek2 in a dose-dependent manner at concentrations of 100 and 1000 nM; however, it had no effect at 10 nM (Figure 3B). The same phenomenon was also observed in MDA-MB-468 cells treated with **32** at 100 nM (Figure 3C, lane 2). Compounds **1** and **2** are reported to induce Nek2 degradation at concentrations of 25 and 6.25 μM, respectively.^{16,17}

As shown in Figure 3C, Nek2 degradation in **32**-treated MDA-MB-468 cells was blocked by the addition of proteasomal inhibitor MG132 (lane 3). MG132 did not interfere with Hec1/Nek2 interaction (Figure 3A, lane 5), nor did it impact the ability of **32** to disrupt Hec1/Nek2 interaction (Figure 3A, lane 4). Taken together, these results suggested that **32** disrupted the Hec1/Nek2 complex in the cells and that the detached Nek2 might be degraded through the proteasomal pathway, as reported by Fry et al.^{21,22}

Hec1 plays a critical role in mitosis, and intervening in its function leads to mitotic abnormalities.^{16,17} In MDA-MB-468 cells treated with **32**, the percentage of mitotic abnormalities, including chromosomal misalignment and formation of multipolar spindles, was measured by immunofluorescent staining and microscopy (Table 5). The percentage of cells displaying multipolar spindles increased in a dose-dependent manner: 16.9, 29.1, and 46.7% for cells treated with **32** at concentrations of 10, 100, and 1000 nM, respectively. However, no significant

Table 3. In Vitro Potency of 4-Aryl-N-(4-pyridylcarbonyl)-2-aminothiazole 13–15, 18, and 32 Bearing a C-4' Alkoxy or Aryloxy, C-2' Methyl or Fluoro, and *o*-Hydro or Fluoro or Chloro at the Pyridyl Group

compd	structure	antiproliferative IC ₅₀ (nM) ^a			
		HeLa	K562	MB468	MB231
13		312	217	450	170
14		75.4	202	220	130
15		203	241	280	160
18		167	42.7	112	61.0
32		42.7	16.3	40.0	20.0

^aThe IC₅₀ values were averaged from two independent dose–response curves; variation was generally <15%.

Table 4. Pharmacokinetic Parameters (IV, PO) of Compounds 9a, 12, 17, 31, and 32^a

compd	MB231 IC ₅₀ (nM)	IV ^b			PO ^c
		AUC (μM·h) ^b	V _d (L/kg)	CL (mL/min/kg)	F%
9a	300	5.78	1.54	23.2	41.9
12	160	32.7	0.250	3.02	20.6
17	96.0	44.3	0.769	2.55	22.6
31	32.0	34.3	1.26	2.70	12.4
32	20.0	64.9	0.948	1.22	4.6 (22.7) ^d

^aCarried out in Sprague–Dawley rats. ^bIV dose: 2.0 mg/kg formulated with 5% DMSO, 10% cremophor, and 85% water. ^cPO dose: 20 mg/kg formulated with 1% methylcellulose in water. ^dFormulated with 5% DMSO, 10% cremophor, and 85% water.

change in the percentage of cells with chromosomal misalignment was observed. These data indicated that **32** induced mitotic abnormalities in the same manner as **1** and **2**, even at a concentration as low as 10 nM (IC₅₀ of **32** for MDA-MB-468: 40.0 nM, Table 3). Furthermore, reduced levels of antiapoptotic proteins, including Bcl-2, Mcl-1, and XIAP, were observed in HeLa cells treated with **32** for 24 and 48 h, whereas increasing levels of apoptotic marker proteins, including cleaved caspase-3 and PARP, were noted (Figure 4). Combined with the results from coimmunoprecipitation, immunofluorescent staining, and western blotting, we propose that antiproliferative compound **32** acted by disrupting the Hec1/Nek2 interaction, which led to mitotic abnormalities and eventually to the apoptosis of the cancer cells.

Spectrum and Selectivity. To further evaluate the spectrum of activity for Hec1/Nek2 inhibition within distinct cancer cells, the GI₅₀ values of **32** were determined. The results shown in Table 6 indicated that **32** was active toward various cancer cells, including CML, lymphoma, cervical cancer, colon cancer, breast cancer, and hepatoma, with GI₅₀ values less than 1.0 μM (22.8–377 nM). The observed broad spectrum activity of **32** toward various cancer cells was anticipated because Hec1 plays a critical role in mitosis. On the contrary, compound **32** was not active (GI₅₀ > 9.0 μM, Table 6) on normal cells, including WI-38 (human normal lung fibroblast), RPTEC (renal proximal tubule epithelial), HUVEC (human umbilical vein endothelial), and HAoSMC (human aortic smooth muscle) cells. These results suggested that compound **32** selectively killed cancer cells over normal cells. The differences

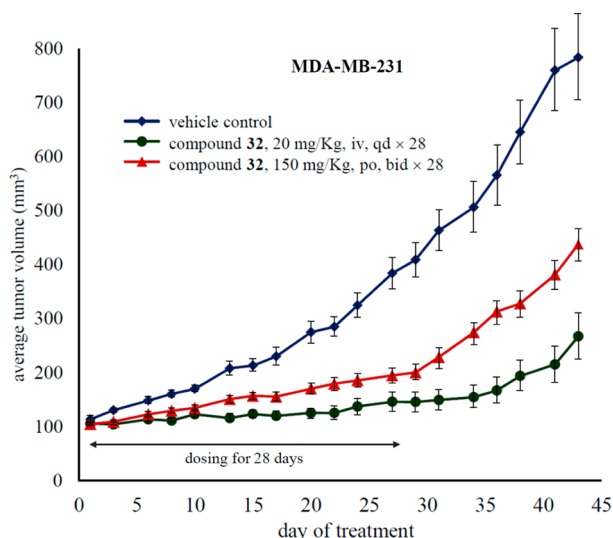


Figure 2. In vivo antitumor activity of compound **32** in nude mice bearing MDA-MB-231 breast cancer xenografts. Compound **32** was formulated with a vehicle of 5% DMSO, 10% cremophor, and 85% water. The average tumor volumes were recorded from mice receiving a 28 day, continuous once-a-day IV dose of the vehicle (\blacklozenge) or **32** at 20 mg/kg (\bullet) as well as from mice receiving a twice-a-day PO dose of **32** at 150 mg/kg (\blacktriangle). The T/C values for **32** from the IV and PO routes were calculated to be 32 and 57% on day 28, respectively.

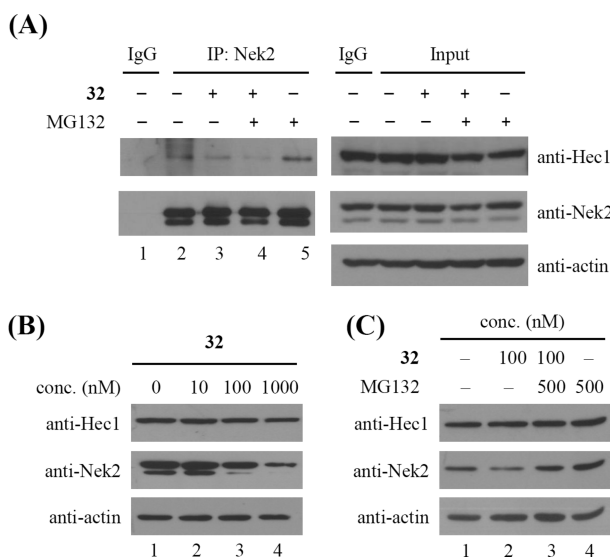


Figure 3. Disruption of Hec1/Nek2 interaction by compound **32** in the cells. (A) Coimmunoprecipitation analysis of K562 cells treated with DMSO (lane 2), **32** (lane 3), **32** with MG132 (lane 4), and MG132 (lane 5) for 16 h. The concentrations of **32** and MG132 were 100 and 500 nM, respectively. (B) Dose-dependent western blot of Hec1 and Nek2 in K562 cells treated with DMSO or **32** at 10, 100, and 1000 nM (lanes 1–4) for 24 h. Actin was used as a loading control. (C) Western blot of Hec1 and Nek2 in MDA-MB-468 cells treated with **32** (lane 2), **32** with MG132 (lane 3), and MG132 (lane 4). Actin was used as a loading control.

in GI_{50} values between cancer and normal cells gave further proof of the good in vivo tolerability of **32** and implied that it has a good therapeutic window.

For further assessment of the selectivity of **32**, radiometric assays²³ were used to address its inhibitory activity against 21 kinases. Compound **32** was not active against Nek2, CHK1,

CHK2, Cdk1/cyclin B, Aurora A, Aurora B, mTOR, PI3K α , PI3K β , VEGFR2, PDGFR- β , FGFR1, EGFR, EGFR(T790M), IGF-1R, B-Raf, B-Raf(V600E), C-Raf, FLT3, MET, and Kit kinases ($IC_{50} > 10 \mu M$), despite sharing a similar 2-aminothiazole structure with the known kinase inhibitor, dasatinib.²⁴ Finally, **32** was inactive in the [³H]astemizole competitive binding assay for hERG liability screening,^{25,26} with an IC_{50} greater than 10 μM . Thus, it is not likely to cause QT prolongation and torsade de pointes²⁷ that often cause the withdrawal of marketed drugs and/or failure in clinical trials. Considering its potency, pharmacokinetic properties, and selectivity, we believe that compound **32** could be a good lead for further optimization.

CONCLUSIONS

We explored 4-aryl-*N*-arylcarbonyl-2-aminothiazoles of scaffold **4** as Hec1/Nek2 inhibitors. Among the derivatives of **4**, compound **32** showed low nanomolar antiproliferative activity, good pharmacokinetic properties, and significant in vivo antitumor activity while being less active toward normal cells, kinases, and hERG. Compound **32** will serve as a good lead in our search for a preclinical candidate targeting Hec1/Nek2 inhibition.

EXPERIMENTAL SECTION

General Procedures. Reagents and starting materials were used as purchased without further purification. Analytical thin-layer chromatography (TLC) was performed on precoated plates (silica gel 60 F-254) purchased from Merck Inc. Purification by gravity column chromatography was conducted using Merck Reagents Silica Gel 60 (with a particle size of 0.063–0.200 mm, 70–230 mesh ASTM). ¹H NMR spectra were recorded on a Bruker (500 MHz) spectrometer with CDCl₃, CD₃OD, or DMSO-*d*₆ as solvent. Multiplicities are abbreviated as follows: s, singlet; d, doublet; t, triplet; q, quartet; and m, multiplet; *J*, coupling constant (hertz). ¹³C NMR spectra were obtained on an Agilent 400-MR (100 MHz) NMR spectrometer by use of CDCl₃ or DMSO-*d*₆ as solvent. ¹³C chemical shifts are referenced to the center peak of CDCl₃ (δ 77.0 ppm) or DMSO-*d*₆ (δ 39.5 ppm). ESI-MS spectra were recorded with an Applied Biosystems API 300 mass spectrometer. High-resolution mass spectra were obtained by means of a LTQ Orbitrap XL mass spectrometer (Thermo Fisher Scientific). The purities of the compounds for biological evaluation were greater than 95%, as determined from reversed-phase HPLC. Reference compound **2**¹⁶ and 1-mesitylethanolone (**6**)¹⁸ were prepared according to reported procedures and showed consistent spectroscopic data.

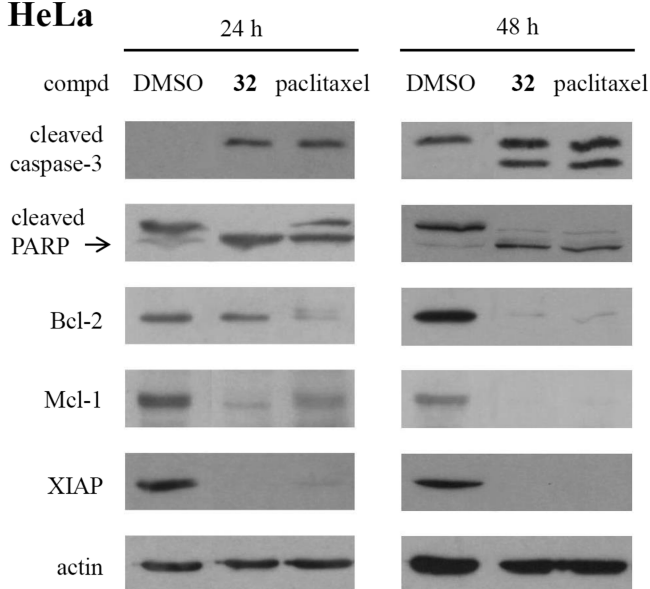
2-Bromo-1-mesitylethanolone (7). To a solution of 1-mesitylethanolone (**6**, 1.18 g, 7.27 mmol) in EtOAc (50 mL) was added CuBr₂ (3.25 g, 14.6 mmol, 2.0 equiv). The reaction mixture was heated at reflux for 90 min. The solution was cooled, and the resultant solids were filtered off and washed with EtOAc. The filtrate was concentrated under reduced pressure to give 2-bromo-1-mesitylethanolone (**7**, 1.67 g, 6.93 mmol) as a yellow oil in 95% yield: ¹H NMR (CDCl₃) δ 6.87 (s, 2H), 4.27 (s, 2H), 2.31 (s, 3H), 2.22 (s, 6H); ¹³C NMR (CDCl₃) δ 200.21, 139.60, 133.51, 128.98, 128.66, 36.67, 21.08, 19.34; ESI-MS: m/z 241.0 (M + H)⁺.

4-Mesitylthiazol-2-amine (8). Compound **7** (2.43 g, 10.1 mmol, 1.0 equiv) and thiourea (0.810 g, 10.6 mmol, 1.05 equiv) were dissolved in 95% ethanol (20 mL). The reaction mixture was heated at reflux for 2.0 h. The solution was concentrated under reduced pressure, and the residue was recrystallized from 2-propanol to give 4-mesitylthiazol-2-amine (**8**, 1.99 g, 9.12 mmol) as white solids in 90% yield: ¹H NMR (CD₃OD) δ 7.00 (s, 2H), 6.67 (s, 1H), 2.31 (s, 3H), 2.19 (s, 6H); ¹³C NMR (CDCl₃) δ 167.66, 137.55, 137.34, 131.96, 128.50, 128.06, 105.12, 21.08, 20.25; ESI-MS: m/z 219.1 (M + H)⁺.

1-(4-Chloro-2,6-dimethylphenyl)ethanolone (22). Anhydrous CuCl₂ (98.9 g, 0.736 mol, 1.2 equiv) was mixed with *t*-BuONO

Table 5. Immunofluorescent Staining (Microscopy, 1000×), Percentage of Chromosomal Misalignment, and Formation of Multipolar Spindles in Mitotic MDA-MB-468 Cells Treated with 32 at Various Concentrations for 48 h

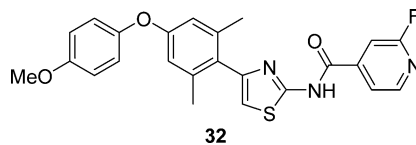
immunofluorescent staining and microscopy			conc. of 32 (nM)	chromosomal misalignment (%)	multipolar spindles (%)	
	α -tubulin	DAPI	merge			
control				– ^a	21.4	5.7
32 (1,000 nM)				10	23.9	16.9
				100	21.8	29.1
				1,000	20.0	46.7

^aDMSO (control).**HeLa****Figure 4.** Western blot analysis of cleaved caspase-3, cleaved PARP, Bcl-2, Mcl-1, and XIAP in HeLa cells treated with DMSO, compound **32** (1.0 μ M), or paclitaxel (100 nM) for 24 and 48 h. Actin was used as a loading control.

(85.6 g, 0.830 mol, 1.4 equiv) in CH_3CN (1.02 L). The solution was cooled to 0 °C, and 1-(4-amino-2,6-dimethylphenyl)ethanone (**21**, 100 g, 0.613 mol, 1.0 equiv) was slowly added over a period of 5.0 min. After the addition was completed, the reaction mixture was warmed to room temperature and poured into an aqueous hydrochloric acid solution (20%, 1.0 L). The solution was extracted with EtOAc (800 mL), and the organic layer was separated, washed with H_2O (1.0 L), dried over $\text{MgSO}_4(\text{s})$, and concentrated under reduced pressure. The liquid was distilled to give 1-(4-chloro-2,6-dimethylphenyl)ethanone (**22**, 85.0 g, 0.465 mol) as a yellow oil in 76% yield: $^1\text{H NMR}$ (CDCl_3) δ 7.02 (s, 2H), 2.45 (s, 3H), 2.22 (s, 6H); $^{13}\text{C NMR}$ (CDCl_3) δ 207.29, 140.87, 134.28, 133.92, 127.66, 77.33, 77.02, 76.70, 32.03, 19.07, 18.98; ESI-MS: m/z 183.0 ($\text{M} + \text{H}$)⁺.

General Procedure for the Synthesis of 4-Aryloxy-2,6-dimethylacetophenones 23a–i. To a solution of 1-(4-chloro-2,6-dimethylphenyl)ethanone (**22**, 1.0 equiv), K_3PO_4 (2.0 equiv), and various aryl alcohols (1.2 equiv) in toluene were added *t*-BuXPhos (0.030 equiv) and $\text{Pd}(\text{OAc})_2$ (0.050 equiv). The reaction mixture was heated at 100 °C for 2.0 h under N_2 . The solution was cooled to room temperature and filtered through a small pad of Celite. The cake was washed with EtOAc, and the combined filtrate was concentrated under reduced pressure. The residue was purified by gravity column chromatography on silica gel (mixture of EtOAc and hexanes as eluent) to give corresponding 4-aryloxy-2,6-dimethylacetophenones **23a–i** in 19–86% yields.

1-(2,6-Dimethyl-4-phenoxyphenyl)ethanone (23a). Yield: 68%. $^1\text{H NMR}$ (CDCl_3) δ 7.33–7.37 (m, 2H), 7.12 (t, $J = 7.5$ Hz, 1H), 7.00 (d, $J = 7.5$ Hz, 2H), 6.65 (s, 2H), 2.48 (s, 3H), 2.22 (s, 6H);

Table 6. GI₅₀ Values of Compound 32 toward Various Cancer and Normal Cells

cell	origin	GI ₅₀ (nM) ^a	cell	origin	GI ₅₀ ^a
K562	CML	56.2	Huh7	hepatoma	79.6 nM
U937	lymphoma	29.6	PLC/PRF/5	hepatoma	79.6 nM
HeLa	cervical	22.8	HepG2	hepatoma	191 nM
HCT116	colon	34.1	Hep3B	hepatoma	68.3 nM
COLO205	colon	35.4	WI-38	normal	>9.0 μ M
MB231	breast	39.8	RPTEC	normal	>9.0 μ M
MB468	breast	29.6	HUVEC	normal	>9.0 μ M
T47D	breast	377	HAoSMC	normal	>9.0 μ M

^aThe GI₅₀ values were averaged from two independent dose–response curves; variation was generally <15%.

^{13}C NMR (CDCl_3) δ 207.66, 157.21, 156.72, 137.74, 134.70, 129.79, 123.53, 119.20, 117.71, 32.25, 19.37; ESI-MS: m/z 241.1 ($\text{M} + \text{H}$) $^+$.

1-[2,6-Dimethyl-4-(*p*-toloxy)phenyl]ethanone (23b). Yield: 46%. ^1H NMR (CDCl_3) δ 7.15 (d, $J = 8.4$ Hz, 2H), 6.91 (d, $J = 8.4$ Hz, 2H), 6.62 (s, 2H), 2.66 (s, 3H), 2.35 (s, 3H), 2.21 (s, 6H); ^{13}C NMR (CDCl_3) δ 207.99, 157.75, 154.12, 137.29, 134.61, 133.23, 130.26, 119.40, 117.14, 32.31, 20.71, 19.39; ESI-MS: m/z 255.3 ($\text{M} + \text{H}$) $^+$.

1-[4-(4-Ethylphenoxy)-2,6-dimethylphenyl]ethanone (23c). Yield: 82%. ^1H NMR (CDCl_3) δ 7.17 (d, $J = 8.5$ Hz, 2H), 6.93 (d, $J = 8.5$ Hz, 2H), 6.63 (s, 2H), 2.64 (q, $J = 7.5$ Hz, 2H), 2.47 (s, 3H), 2.21 (s, 6H), 1.25 (t, $J = 7.5$ Hz, 3H); ^{13}C NMR (CDCl_3) δ 207.92, 157.69, 154.34, 139.58, 137.35, 134.62, 129.06, 119.33, 117.26, 32.31, 28.16, 19.40, 15.68; ESI-MS: m/z 269.2 ($\text{M} + \text{H}$) $^+$.

1-[4-(3,5-Dimethylphenoxy)-2,6-dimethylphenyl]ethanone (23d). Yield: 86%. ^1H NMR (CDCl_3) δ 6.76 (s, 1H), 6.63 (s, 2H), 6.62 (s, 2H), 2.48 (s, 3H), 2.29 (s, 6H), 2.22 (s, 6H); ^{13}C NMR (CDCl_3) δ 208.03, 157.39, 156.67, 139.59, 137.48, 134.58, 125.23, 117.72, 116.85, 32.28, 21.26, 19.37; ESI-MS: m/z 269.1 ($\text{M} + \text{H}$) $^+$.

1-[4-(4-Fluorophenoxy)-2,6-dimethylphenyl]ethanone (23e). Yield: 68%. ^1H NMR (CDCl_3) δ 7.01–7.05 (m, 2H), 6.70–6.96 (m, 2H), 6.60 (s, 2H), 2.47 (s, 3H), 2.22 (s, 6H); ^{13}C NMR (CDCl_3) δ 207.68, 158.89 (d, $J = 262.4$ Hz), 157.53, 152.33, 137.58, 134.76, 120.84 (d, $J = 8.3$ Hz), 117.09, 116.32 (d, $J = 23.2$ Hz), 32.28, 19.39; ESI-MS: m/z 259.0 ($\text{M} + \text{H}$) $^+$.

1-[2,6-Dimethyl-4-[4-(trifluoromethyl)phenoxy]phenyl]ethanone (23f). Yield: 19%. ^1H NMR (CDCl_3) δ 7.58 (d, $J = 8.5$ Hz, 2H), 7.04 (d, $J = 8.5$ Hz, 2H), 6.70 (s, 2H), 2.50 (s, 3H), 2.25 (s, 6H); ^{13}C NMR (CDCl_3) δ 207.66, 160.05, 155.58, 138.89, 135.01, 127.11 (q, $J = 3.7$ Hz), 126.60 (q, $J = 215$ Hz), 125.06 (q, $J = 32.6$ Hz), 118.79, 118.13, 32.18, 19.28; ESI-MS: m/z 309.0 ($\text{M} + \text{H}$) $^+$.

1-[4-(4-Methoxyphenoxy)-2,6-dimethylphenyl]ethanone (23g). Yield: 75%. ^1H NMR (CDCl_3) δ 6.96 (d, $J = 9.2$ Hz, 2H), 6.88 (d, $J = 9.2$ Hz, 2H), 6.57 (s, 2H), 3.81 (s, 3H), 2.46 (s, 3H), 2.20 (s, 6H); ^{13}C NMR ($\text{DMSO}-d_6$) δ 207.63, 158.21, 156.22, 149.32, 137.50, 134.85, 121.42, 116.42, 115.52, 55.80, 32.58, 19.33; ESI-MS: m/z 271.1 ($\text{M} + \text{H}$) $^+$.

1-[4-(3-Methoxyphenoxy)-2,6-dimethylphenyl]ethanone (23h). Yield: 73%. ^1H NMR (CDCl_3) δ 7.23–7.25 (m, 1H), 6.66–6.68 (m, 3H), 6.56–6.57 (m, 2H), 3.79 (s, 3H), 2.48 (s, 3H), 2.22 (s, 6H); ^{13}C NMR (CDCl_3) δ 207.89, 160.95, 157.91, 156.94, 137.81, 134.66, 130.15, 117.86, 111.26, 109.11, 105.18, 55.34, 32.27, 19.36; ESI-MS: m/z 271.0 ($\text{M} + \text{H}$) $^+$.

1-[4-(Benzo[d][1,3]dioxol-5-yloxy)-2,6-dimethylphenyl]ethanone (23i). Yield: 62%. ^1H NMR (CDCl_3) δ 6.77 (d, $J = 8.5$ Hz, 1H), 6.59 (s, 2H), 6.56 (s, 1H), 6.46–6.49 (m, 1H), 5.98 (s, 2H), 2.46 (s, 3H), 2.21 (s, 6H); ^{13}C NMR (CDCl_3) δ 207.90, 158.10, 150.79, 148.36, 143.96, 137.24, 134.64, 116.67, 112.24, 108.28, 102.35, 101.54, 32.30, 19.41; ESI-MS: m/z 285.1 ($\text{M} + \text{H}$) $^+$.

General Procedure for the Synthesis of 4-Aryl-2-aminothiazoles 11a–f and 24a–i. To a CH_3CN solution of acetylarenes 10a–f or 23a–i (1.0 equiv) was added TBABr_3 (1.0 equiv). The reaction mixture was stirred at room temperature for 80 min. The solution was concentrated under reduced pressure, diluted with H_2O , and extracted with EtOAc . The organic layer was washed with brine, dried over anhydrous $\text{MgSO}_4(\text{s})$, and concentrated under reduced pressure to give the brominated acetylarene. Thiourea (1.0 equiv) was added to the brominated acetylarene in EtOH , and the reaction mixture was heated at reflux for 60 min. After the reaction was completed, the solution was concentrated, and water and saturated aqueous Na_2CO_3 were added. The resultant precipitate was filtered and recrystallized in toluene (50 mL). The solids were collected and dried under vacuum to give the desired 4-aryl-2-aminothiazoles 11a–f or 24a–i in 53–96% yields.

4-(4-Methoxy-2,6-dimethylphenyl)thiazol-2-amine (11a). Yield: 66%. ^1H NMR (CDCl_3) δ 6.61 (s, 2H), 6.27 (s, 1H), 4.91 (bs, 2H), 3.79 (s, 3H), 2.15 (s, 6H); ^{13}C NMR ($\text{DMSO}-d_6$) δ 169.91, 160.36, 139.83, 136.30, 121.33, 113.42, 106.29, 55.69, 20.49; ESI-MS: m/z 235.1 ($\text{M} + \text{H}$) $^+$.

4-(2,6-Difluoro-4-methoxyphenyl)thiazol-2-amine (11b). Yield: 57%. ^1H NMR (CDCl_3) δ 6.68 (s, 1H), 6.51 (d, $J = 10$ Hz, 2H), 5.07 (brs, 2H), 3.81 (s, 3H); ^{13}C NMR ($\text{DMSO}-d_6$) δ 168.22, 160.93 (dd, $J = 245.7, 10.4$ Hz), 160.31 (t, $J = 14.3$ Hz), 138.50, 107.35, 106.30 (t, $J = 18.7$ Hz), 98.70 (dd, $J = 21.4, 7.9$ Hz), 56.30; ESI-MS: m/z 243.2 ($\text{M} + \text{H}$) $^+$.

4-(4-Ethoxy-2,6-dimethylphenyl)thiazol-2-amine (11c). Yield: 72%. ^1H NMR ($\text{DMSO}-d_6$) δ 6.84 (brs, 2H), 6.60 (s, 2H), 6.27 (s, 1H), 3.99 (q, $J = 6.8$ Hz, 2H), 2.06 (s, 6H), 1.31 (t, $J = 6.8$ Hz, 3H); ^{13}C NMR ($\text{DMSO}-d_6$) δ 168.07, 157.83, 149.39, 138.44, 129.14, 113.31, 104.18, 63.14, 20.83, 15.16; ESI-MS: m/z 249.1 ($\text{M} + \text{H}$) $^+$.

4-(4-Isopropoxy-2,6-dimethylphenyl)thiazol-2-amine (11d). Yield: 72%. ^1H NMR (CDCl_3) δ 6.60 (s, 2H), 6.26 (s, 1H), 4.97 (bs, 2H), 4.51–4.56 (m, 1H), 2.13 (s, 6H), 1.32 (d, $J = 6.1$ Hz, 6H); ^{13}C NMR ($\text{DMSO}-d_6$) δ 168.71, 158.73, 138.91, 126.33, 113.57, 104.86, 74.04, 28.18, 20.67, 19.48; ESI-MS: m/z 263.2 ($\text{M} + \text{H}$) $^+$.

4-(4-Isobutoxy-2,6-dimethylphenyl)thiazol-2-amine (11e). Yield: 82%. ^1H NMR (CDCl_3) δ 6.61 (s, 2H), 6.24 (s, 1H), 3.70 (d, $J = 6.5$ Hz, 2H), 2.15 (s, 6H), 2.05–2.09 (m, 1H), 1.01 (d, $J = 6.7$ Hz, 6H); ^{13}C NMR (CDCl_3) δ 167.55, 158.68, 148.83, 138.92, 127.16, 113.27, 105.30, 74.27, 28.28, 20.58, 19.28; ESI-MS: m/z 277.0 ($\text{M} + \text{H}$) $^+$.

4-[4-(Cyclopentyloxy)-2,6-dimethylphenyl]thiazol-2-amine (11f). Yield: 74%. ^1H NMR (CDCl_3) δ 6.58 (s, 2H), 6.24 (s, 1H), 4.73–4.77 (m, 1H), 2.13 (s, 6H), 1.78–1.88 (m, 6H), 1.59–1.62 (m, 2H); ^{13}C NMR ($\text{DMSO}-d_6$) δ 168.17, 157.03, 148.47, 138.48, 128.35, 114.35, 104.27, 78.69, 32.78, 24.04, 20.80; ESI-MS: m/z 289.1 ($\text{M} + \text{H}$) $^+$.

4-(2,6-Dimethyl-4-phenoxyphenyl)thiazol-2-amine (24a). Yield: 59%. ^1H NMR (CDCl_3) δ 7.31–7.35 (m, 2H), 7.10–7.26 (m, 3H), 6.72 (s, 2H), 6.30 (s, 1H), 5.18 (bs, 2H), 2.14 (s, 6H); ^{13}C NMR ($\text{DMSO}-d_6$) δ 168.49, 157.14, 156.11, 147.70, 139.39, 131.47, 130.39, 123.72, 119.07, 117.51, 104.63, 20.66; ESI-MS: m/z 297.1 ($\text{M} + \text{H}$) $^+$.

4-[2,6-Dimethyl-4-(*p*-toloxy)phenyl]thiazol-2-amine (24b). Yield: 53%. ^1H NMR ($\text{DMSO}-d_6$) δ 7.23 (d, $J = 8.3$ Hz, 2H), 6.94 (d, $J = 8.3$ Hz, 2H), 6.75 (br, 3H), 2.36 (s, 3H), 2.12 (s, 6H); ^{13}C NMR ($\text{DMSO}-d_6$) δ 170.00, 158.66, 153.83, 140.50, 135.96, 133.66, 130.99, 123.74, 119.86, 116.90, 106.53, 20.77, 20.39; ESI-MS: m/z 311.2 ($\text{M} + \text{H}$) $^+$.

4-[4-(4-Ethylphenoxy)-2,6-dimethylphenyl]thiazol-2-amine (24c). Yield: 88%. ^1H NMR (CDCl_3) δ 7.18 (d, $J = 8.0$ Hz, 2H), 6.95 (d, $J = 8.0$ Hz, 2H), 6.71 (s, 2H), 6.29 (s, 1H), 5.45 (bs, 2H), 2.64 (q, $J = 7.6$ Hz, 2H), 2.14 (s, 6H), 1.25 (t, $J = 7.6$ Hz, 3H); ^{13}C NMR (CDCl_3) δ 167.56, 157.21, 154.80, 147.77, 139.42, 139.19, 134.63, 128.96, 119.07, 117.13, 105.57, 28.14, 20.48, 15.70; ESI-MS: m/z 325.0 ($\text{M} + \text{H}$) $^+$.

4-[4-(3,5-Dimethylphenoxy)-2,6-dimethylphenyl]thiazol-2-amine (24d). Yield: 59%. ^1H NMR (CDCl_3) δ 6.76 (s, 1H), 6.68 (s, 2H), 6.64 (s, 2H), 6.26 (s, 1H), 2.29 (s, 6H), 2.16 (s, 6H); ^{13}C NMR ($\text{DMSO}-d_6$) δ 168.77, 156.94, 156.77, 139.73, 139.51, 129.64, 125.50, 119.21, 117.44, 116.89, 104.99, 21.31, 20.59; ESI-MS: m/z 325.1 ($\text{M} + \text{H}$) $^+$.

4-[4-(4-Fluorophenoxy)-2,6-dimethylphenyl]thiazol-2-amine (24e). Yield: 84%. ^1H NMR (CDCl_3) δ 6.97–7.05 (m, 4H), 6.66 (s, 2H), 6.28 (s, 1H), 5.95 (bs, 2H), 2.14 (s, 6H); ^{13}C NMR ($\text{DMSO}-d_6$) δ 168.96, 158.69 (d, $J = 238$ Hz), 157.18, 152.80 (d, $J = 2.3$ Hz), 143.54, 139.84, 128.90, 121.26 (d, $J = 8.5$ Hz), 117.04 (d, $J = 23.2$ Hz), 117.00, 105.27, 20.54; ESI-MS: m/z 315.1 ($\text{M} + \text{H}$) $^+$.

4-[2,6-Dimethyl-4-[4-(trifluoromethyl)phenoxy]phenyl]thiazol-2-amine (24f). Yield: 63%. ^1H NMR (CDCl_3) δ 7.56 (d, $J = 8.5$ Hz, 2H), 7.05 (d, $J = 8.5$ Hz, 2H), 6.76 (s, 2H), 6.32 (s, 1H), 5.03 (brs, 2H), 2.17 (s, 6H); ^{13}C NMR ($\text{DMSO}-d_6$) δ 168.48, 160.92, 154.28, 148.40, 139.73, 133.38, 127.68, 124.69 (q, $J = 207$ Hz), 123.66 (q, $J = 32.1$ Hz), 118.68, 118.20, 104.51, 20.55; ESI-MS: m/z 365.1 ($\text{M} + \text{H}$) $^+$.

4-[4-(4-Methoxyphenoxy)-2,6-dimethylphenyl]thiazol-2-amine (24g). Yield: 68%. ^1H NMR (CDCl_3) δ 6.98 (d, $J = 9.0$ Hz, 2H), 6.88 (d, $J = 9.0$ Hz, 2H), 6.64 (s, 2H), 6.27 (s, 1H), 5.40 (bs, 2H), 3.81 (s, 3H), 2.13 (s, 6H); ^{13}C NMR ($\text{DMSO}-d_6$) δ 168.36,

157.47, 155.99, 149.83, 147.77, 139.17, 130.62, 121.15, 116.19, 115.46, 104.59, 55.80, 20.67; ESI-MS: m/z 327.1 (M + H)⁺.

4-[4-(3-Methoxyphenoxy)-2,6-dimethylphenyl]thiazol-2-amine (24h). Yield: 65%. ¹H NMR (CDCl₃) δ 7.20–7.23 (m, 1H), 6.64 (s, 2H), 6.60–6.63 (m, 1H), 6.45–6.50 (m, 2H), 6.30 (s, 1H), 3.81 (s, 3H), 1.94 (s, 6H); ¹³C NMR (DMSO-*d*₆) δ 168.43, 161.10, 158.41, 155.79, 148.74, 139.27, 132.14, 130.78, 117.60, 110.99, 109.21, 105.17, 104.45, 55.57, 20.66; ESI-MS: m/z 327.0 (M + H)⁺.

4-[4-(Benzo[*d*][1,3]dioxol-5-yloxy)-2,6-dimethylphenyl]thiazol-2-amine (24i). Yield: 96%. ¹H NMR (CDCl₃) δ 6.75 (d, *J* = 8.5 Hz, 1H), 6.66 (s, 2H), 6.57–6.59 (m, 1H), 6.48–6.51 (m, 1H), 6.28 (s, 1H), 5.98 (s, 2H), 5.05 (brs, 2H), 2.13 (s, 6H); ¹³C NMR (DMSO-*d*₆) δ 168.19, 157.06, 151.16, 148.57, 143.94, 139.09, 131.46, 116.56, 116.32, 112.22, 108.84, 104.45, 102.45, 101.98, 20.69; ESI-MS: m/z 341.0 (M + H)⁺.

General Procedure for the Synthesis of 4-Aryl-*N*-acyl-2-aminothiazoles 9a–e, 12–20, and 25–34. To a solution of 4-aryl-2-aminothiazoles **8** or **11a–f** or **24a–i** (1.0 equiv) in anhydrous CH₂Cl₂ was added DMAP (3.0 equiv) followed by various acyl chlorides (1.5 equiv) under N₂. The reaction mixture was stirred at room temperature for 12 h. The solution was concentrated under reduced pressure, and hot water was added. After cooling, the resultant precipitate was filtered, dried under vacuum, and purified by gravity column chromatography on silica gel (mixture of EtOAc and hexanes as eluent) to give the corresponding 4-aryl-*N*-acyl-2-aminothiazoles **9a–e**, **12–20**, and **25–34** in 17–99% yields.

***N*-(4-Mesitylthiazol-2-yl)isonicotinamide (9a).** Yield: 77%. ¹H NMR (CD₃OD) δ 8.72 (d, *J* = 6.0 Hz, 2H), 7.56 (d, *J* = 6.0 Hz, 2H), 6.80 (s, 1H), 6.65 (s, 2H), 2.20 (s, 3H), 1.94 (s, 6H); ¹³C NMR (CDCl₃) δ 163.75, 159.23, 149.91, 148.11, 138.48, 137.76, 136.55, 130.48, 128.24, 120.94, 112.02, 77.34, 77.02, 76.70, 20.83, 20.11; ESI-MS: m/z 324.0 (M + H)⁺; HRMS calcd for C₁₈H₁₈N₃OS (M⁺ + H), 324.1168; found, 324.1165.

***N*-(4-Mesitylthiazol-2-yl)-2-(pyridin-4-yl)acetamide (9b).** Yield: 65%. ¹H NMR (DMSO-*d*₆) δ 8.53 (d, *J* = 5.8 Hz, 2H), 7.36 (d, *J* = 5.8 Hz, 2H), 6.99 (s, 1H), 6.91 (s, 2H), 3.84 (s, 2H), 2.25 (s, 3H), 2.02 (s, 6H); ¹³C NMR (CDCl₃) δ 167.88, 158.87, 149.84, 147.76, 142.34, 138.39, 137.39, 131.58, 128.70, 124.63, 111.72, 77.30, 76.98, 76.67, 40.34, 21.00, 20.32; ESI-MS: m/z 338.1 (M + H)⁺.

4-Cyano-*N*-(4-mesitylthiazol-2-yl)benzamide (9c). Yield: 67%. ¹H NMR (DMSO-*d*₆) δ 8.23 (d, *J* = 8.4 Hz, 2H), 8.03 (d, *J* = 8.4 Hz, 2H), 7.09 (s, 1H), 6.92 (s, 2H), 2.26 (s, 3H), 2.05 (s, 6H); ¹³C NMR (CDCl₃) δ 163.58, 159.72, 146.46, 138.35, 136.74, 135.00, 132.03, 129.31, 128.39, 128.30, 117.75, 116.04, 111.89, 20.94, 20.23; ESI-MS: m/z 348.0 (M + H)⁺.

4-[4-(4-Mesitylthiazol-2-yl)carbamoyl]pyridine 1-Oxide (9d). Yield: 75%. ¹H NMR (CDCl₃) δ 8.16 (d, *J* = 6.6 Hz, 2H), 7.79 (d, *J* = 6.6 Hz, 2H), 6.83 (s, 1H), 6.80 (s, 2H), 2.23 (s, 3H), 2.01 (s, 6H); ¹³C NMR (CDCl₃) δ 161.95, 159.63, 147.51, 138.82, 138.14, 136.85, 130.70, 128.58, 128.08, 124.50, 112.03, 77.35, 77.03, 76.71, 20.88, 20.06; ¹³C NMR (CDCl₃) δ 161.95, 159.63, 147.51, 138.82, 138.14, 136.85, 130.70, 128.58, 128.08, 124.50, 112.03, 77.35, 77.03, 76.71, 20.88, 20.06; ESI-MS: m/z 340.1 (M + H)⁺.

2-Chloro-*N*-(4-mesitylthiazol-2-yl)isonicotinamide (9e). Yield: 87%. ¹H NMR (DMSO-*d*₆) δ 8.50 (d, *J* = 5.1 Hz, 1H), 7.74 (d, *J* = 5.1 Hz, 1H), 7.62 (s, 1H), 6.83 (s, 1H), 6.72 (s, 2H), 2.26 (s, 3H), 1.97 (s, 6H); ¹³C NMR (CDCl₃) δ 162.76, 159.58, 152.25, 149.59, 147.67, 141.60, 138.29, 136.62, 130.02, 128.23, 122.38, 119.65, 112.18, 20.98, 20.12; ESI-MS: m/z 357.9 (M + H)⁺.

***N*-(4-(4-Methoxy-2,6-dimethylphenyl)thiazol-2-yl)isonicotinamide (12).** Yield: 69%. ¹H NMR (CDCl₃) δ 8.70 (d, *J* = 6.0 Hz, 2H), 7.56 (d, *J* = 6.0 Hz, 2H), 6.81 (s, 1H), 6.36 (s, 2H), 3.76 (s, 3H), 1.92 (s, 6H); ¹³C NMR (CDCl₃) δ 163.88, 159.40, 158.89, 149.86, 147.65, 138.80, 138.23, 125.73, 121.14, 112.81, 112.12, 54.92, 20.43; ESI-MS: m/z 340.0 (M + H)⁺.

***N*-(4-(2,6-Difluoro-4-methoxyphenyl)thiazol-2-yl)isonicotinamide (13).** Yield: 49%. ¹H NMR (DMSO-*d*₆) δ 13.13 (s, 1H), 8.81 (d, *J* = 5.9 Hz, 2H), 8.00 (d, *J* = 5.9 Hz, 2H), 7.46 (s, 1H), 6.87 (d, *J* = 10 Hz, 2H), 3.83 (s, 3H); ¹³C NMR (CDCl₃) δ 164.39, 160.99 (t, *J* = 14.3 Hz), 160.89 (dd, *J* = 245.7, 10.2 Hz), 158.03,

151.20, 150.84, 139.56, 122.23, 115.26, 105.48 (t, *J* = 19.0 Hz), 99.02 (dd, *J* = 21.2, 7.9 Hz), 56.62; ESI-MS: m/z 348.1 (M + H)⁺.

2-Fluoro-*N*-(4-(4-methoxy-2,6-dimethylphenyl)thiazol-2-yl)isonicotinamide (14). Yield: 68%. ¹H NMR (CDCl₃) δ 8.37 (d, *J* = 5.2 Hz, 1H), 7.72 (brs, 1H), 7.42 (d, *J* = 5.2 Hz, 1H), 6.84 (s, 1H), 6.48 (s, 2H), 3.78 (s, 3H), 2.03 (s, 6H); ¹³C NMR (CDCl₃) δ 163.87 (d, *J* = 242.2 Hz), 162.69, 159.45, 159.07, 147.96 (d, *J* = 14.5 Hz), 147.58, 144.13 (d, *J* = 7.5 Hz), 138.31, 125.41, 118.97 (d, *J* = 4.4 Hz), 112.79, 112.38, 107.98 (d, *J* = 39.1 Hz), 54.88, 20.34; ESI-MS: m/z 358.0 (M + H)⁺; HRMS calcd for C₁₈H₁₇FN₃O₂S (M⁺ + H), 358.1015; found, 358.1020.

2-Chloro-*N*-(4-(4-methoxy-2,6-dimethylphenyl)thiazol-2-yl)isonicotinamide (15). Yield: 63%. ¹H NMR (CDCl₃) δ 8.60 (d, *J* = 5.1 Hz, 1H), 7.95 (s, 1H), 7.92 (d, *J* = 5.1 Hz, 1H), 6.87 (s, 1H), 6.58 (s, 2H), 3.81 (s, 3H), 2.11 (s, 6H); ¹³C NMR (CDCl₃) δ 162.82, 159.61, 159.16, 152.17, 149.80, 147.41, 141.68, 138.35, 125.32, 122.34, 119.77, 112.78, 112.30, 54.98, 20.45; ESI-MS: m/z 373.9 (M + H)⁺.

***N*-(4-(4-Ethoxy-2,6-dimethylphenyl)thiazol-2-yl)isonicotinamide (16).** Yield: 88%. ¹H NMR (CDCl₃) δ 8.70 (d, *J* = 6.0 Hz, 2H), 7.58 (d, *J* = 6.0 Hz, 2H), 6.78 (s, 1H), 6.37 (s, 2H), 3.95 (q, *J* = 7.0 Hz, 2H), 1.94 (s, 6H), 1.41 (t, *J* = 7.0 Hz, 3H); ¹³C NMR (CDCl₃) δ 163.76, 159.09, 158.34, 150.10, 147.98, 138.60, 138.18, 125.68, 121.00, 113.34, 112.13, 63.06, 20.45, 14.88; ESI-MS: m/z 353.6 (M + H)⁺.

***N*-(4-(4-Isopropoxy-2,6-dimethylphenyl)thiazol-2-yl)isonicotinamide (17).** Yield: 80%. ¹H NMR (CDCl₃) δ 8.67 (d, *J* = 6.0 Hz, 2H), 7.55 (d, *J* = 6.0 Hz, 2H), 6.77 (s, 1H), 6.30 (s, 2H), 4.41–4.45 (m, 1H), 1.90 (s, 6H), 1.32 (d, *J* = 6.0 Hz, 6H); ¹³C NMR (CDCl₃) δ 163.75, 159.05, 157.36, 150.09, 148.01, 138.62, 138.20, 125.54, 121.02, 114.35, 112.15, 69.27, 22.13, 20.49; ESI-MS: m/z 368.1 (M + H)⁺.

2-Fluoro-*N*-(4-(4-isopropoxy-2,6-dimethylphenyl)thiazol-2-yl)isonicotinamide (18). Yield: 83%. ¹H NMR (CDCl₃) δ 8.40 (d, *J* = 5.1 Hz, 1H), 7.78 (s, 1H), 7.50 (d, *J* = 5.1 Hz, 1H), 6.84 (s, 1H), 6.53 (s, 2H), 4.52–4.56 (m, 1H), 2.06 (s, 6H), 1.33 (d, *J* = 6.0 Hz, 6H); ¹³C NMR (CDCl₃) δ 163.89 (d, *J* = 241.3 Hz), 162.72, 159.47, 157.52, 147.91 (d, *J* = 14.5 Hz), 147.61, 144.13 (d, *J* = 7.5 Hz), 138.29, 125.05, 118.99 (d, *J* = 4.4 Hz), 114.21, 112.29, 108.06 (d, *J* = 39.1 Hz), 69.24, 22.04, 20.39; ESI-MS: m/z 385.8 (M + H)⁺.

***N*-(4-(4-Isobutoxy-2,6-dimethylphenyl)thiazol-2-yl)isonicotinamide (19).** Yield: 99%. ¹H NMR (CDCl₃) δ 8.68 (d, *J* = 5.7 Hz, 2H), 7.56 (d, *J* = 5.7 Hz, 2H), 6.77 (s, 1H), 6.33 (s, 2H), 3.62 (d, *J* = 6.5 Hz, 2H), 2.05–2.12 (m, 1H), 1.91 (s, 6H), 1.05 (d, *J* = 6.7 Hz, 6H); ¹³C NMR (CDCl₃) δ 163.78, 159.16, 158.65, 150.07, 147.95, 138.59, 138.16, 125.52, 121.04, 113.30, 112.08, 73.99, 28.29, 20.42, 19.29; ESI-MS: m/z 382.1 (M + H)⁺.

***N*-(4-(4-(Cyclopentyloxy)-2,6-dimethylphenyl)thiazol-2-yl)isonicotinamide (20).** Yield: 62%. ¹H NMR (CDCl₃) δ 8.71 (d, *J* = 5.8 Hz, 2H), 7.60 (d, *J* = 5.8 Hz, 2H), 6.78 (s, 1H), 6.37 (s, 2H), 4.65–4.69 (m, 1H), 1.95 (s, 6H), 1.52–1.94 (m, 8H); ¹³C NMR (CDCl₃) δ 163.71, 159.06, 157.61, 150.13, 148.01, 138.62, 138.14, 125.32, 121.04, 114.26, 112.11, 78.77, 32.86, 23.94, 20.51; ESI-MS: m/z 394.1 (M + H)⁺.

***N*-(4-(2,6-Dimethyl-4-phenoxyphenyl)thiazol-2-yl)isonicotinamide (25).** Yield: 30%. ¹H NMR (DMSO-*d*₆) δ 8.81 (d, *J* = 5.5 Hz, 2H), 7.99 (d, *J* = 5.5 Hz, 2H), 7.39–7.42 (m, 2H), 7.03–7.19 (m, 4H), 6.78 (s, 2H), 2.07 (s, 6H); ¹³C NMR (CDCl₃) δ 163.74, 159.08, 156.93, 156.43, 150.33, 147.66, 138.75, 129.78, 128.31, 123.56, 121.04, 119.32, 117.17, 112.40, 77.36, 77.05, 76.73, 20.43; ESI-MS: m/z 401.8 (M + H)⁺.

***N*-(4-[2,6-Dimethyl-4-(*p*-tolylloxy)phenyl]thiazol-2-yl)isonicotinamide (26).** Yield: 89%. ¹H NMR (DMSO-*d*₆) δ 8.80 (d, *J* = 5.5 Hz, 2H), 7.99 (d, *J* = 5.5 Hz, 2H), 7.18–7.22 (m, 3H), 6.95 (d, *J* = 8.4 Hz, 2H), 6.73 (s, 2H), 2.30 (s, 3H), 2.06 (s, 6H); ¹³C NMR (CDCl₃) δ 163.68, 159.02, 157.50, 153.91, 150.37, 147.72, 138.76, 138.70, 133.26, 130.28, 127.91, 121.04, 119.52, 116.66, 112.32, 20.74, 20.43; ESI-MS: m/z 413.9 (M + H)⁺.

***N*-(4-(4-Ethylphenoxy)-2,6-dimethylphenyl)thiazol-2-yl)isonicotinamide (27).** Yield: 91%. ¹H NMR (CDCl₃) δ 8.78 (d, *J* = 6.0 Hz, 2H), 7.67 (d, *J* = 6.0 Hz, 2H), 7.19 (d, *J* = 8.4 Hz, 2H), 6.93 (d, *J* = 8.4 Hz, 2H), 6.83 (s, 1H), 6.56 (s, 2H), 2.66 (q, *J* = 7.6 Hz,

2H), 1.98 (s, 6H), 1.26 (t, $J = 7.6$ Hz, 3H); ^{13}C NMR (CDCl_3) δ 163.72, 159.02, 157.42, 154.04, 150.32, 147.72, 139.63, 138.76, 138.66, 129.07, 127.91, 121.04, 119.46, 116.72, 112.34, 28.17, 20.43, 15.67; ESI-MS: m/z 429.6 ($M + H$) $^+$.

***N*-[4-[4-(3,5-Dimethylphenoxy)-2,6-dimethylphenyl]thiazol-2-yl]isonicotinamide (28)**. Yield: 94%. ^1H NMR (CDCl_3) δ 8.81 (d, $J = 5.4$ Hz, 2H), 7.78 (d, $J = 5.4$ Hz, 2H), 6.84 (s, 1H), 6.78 (s, 1H), 6.64 (s, 2H), 6.61 (s, 2H), 2.31 (s, 6H), 2.02 (s, 6H); ^{13}C NMR (CDCl_3) δ 163.72, 159.29, 157.32, 156.38, 150.03, 147.18, 139.61, 139.32, 138.85, 127.86, 125.36, 121.32, 117.19, 117.05, 112.16, 21.31, 20.45; ESI-MS: m/z 429.8 ($M + H$) $^+$.

***N*-[4-[4-(4-Fluorophenoxy)-2,6-dimethylphenyl]thiazol-2-yl]isonicotinamide (29)**. Yield: 17%. ^1H NMR (CDCl_3) δ 8.72 (d, $J = 6.0$ Hz, 2H), 7.60 (d, $J = 6.0$ Hz, 2H), 7.03–7.07 (m, 2H), 6.93–6.95 (m, 2H), 6.81 (s, 1H), 6.43 (s, 2H), 1.92 (s, 6H); ^{13}C NMR (CDCl_3) δ 163.48, 158.93 (d, $J = 240.8$ Hz), 158.75, 157.30, 152.19 (d, $J = 2.4$ Hz), 150.44, 147.75, 138.91, 138.71, 128.46, 120.95, 120.87 (d, $J = 8.2$ Hz), 116.69, 116.35 (d, $J = 23.2$ Hz), 112.42, 20.45; ESI-MS: m/z 420.2 ($M + H$) $^+$.

***N*-[4-[2,6-Dimethyl-4-[4-(trifluoromethyl)phenoxy]phenyl]thiazol-2-yl]isonicotinamide (30)**. Yield: 87%. ^1H NMR (CDCl_3) δ 8.76 (d, $J = 6.0$ Hz, 2H), 7.64 (d, $J = 6.0$ Hz, 2H), 7.59 (d, $J = 8.6$ Hz, 2H), 7.02 (d, $J = 8.6$ Hz, 2H), 6.86 (s, 1H), 6.57 (s, 2H), 1.98 (s, 6H); ^{13}C NMR (CDCl_3) δ 163.47, 159.87, 158.88, 155.34, 150.47, 147.55, 139.24, 138.61, 129.79, 127.12 (q, $J = 3.8$ Hz), 125.06 (q, $J = 32.6$ Hz), 124.11 (q, $J = 271.5$ Hz), 120.96, 118.35, 118.16, 112.57, 20.43; ESI-MS: m/z 469.7 ($M + H$) $^+$.

***N*-[4-[4-(4-Methoxyphenoxy)-2,6-dimethylphenyl]thiazol-2-yl]isonicotinamide (31)**. Yield: 95%. ^1H NMR (CDCl_3) δ 8.71 (d, $J = 6.0$ Hz, 2H), 7.60 (d, $J = 6.0$ Hz, 2H), 6.90–6.96 (m, 4H), 6.79 (s, 1H), 6.40 (s, 2H), 3.83 (s, 3H), 1.90 (s, 6H); ^{13}C NMR (CDCl_3) δ 163.81, 159.17, 158.09, 156.06, 150.15, 149.26, 147.59, 138.91, 138.63, 127.56, 121.15, 121.12, 115.96, 114.90, 112.32, 55.63, 20.44; ESI-MS: m/z 431.7 ($M + H$) $^+$.

2-Fluoro-*N*-[4-[4-(4-methoxyphenoxy)-2,6-dimethylphenyl]thiazol-2-yl]isonicotinamide (32). Yield: 70%. ^1H NMR (CDCl_3 , 400 MHz) δ 12.51 (brs, 1H), 8.28 (d, $J = 5.2$ Hz, 1H), 7.44 (d, $J = 5.1$ Hz, 1H), 7.22 (s, 1H), 6.96 (d, $J = 9.2$ Hz, 2H), 6.91 (d, $J = 9.2$ Hz, 2H), 6.79 (s, 1H), 6.37 (s, 2H), 3.82 (s, 3H), 1.86 (s, 6H); ^{13}C NMR (CDCl_3) δ 162.02 (d, $J = 239.2$ Hz), 162.45 (d, $J = 3.8$ Hz), 159.07, 158.36, 156.14, 149.16, 148.35 (d, $J = 14.6$ Hz), 147.55, 144.22 (d, $J = 7.5$ Hz), 138.68, 127.18, 121.26, 118.87 (d, $J = 4.6$ Hz), 115.85, 114.92, 112.55, 108.04 (d, $J = 39.1$ Hz), 55.64, 20.35; ESI-MS: m/z 450.0 ($M + H$) $^+$; HRMS calcd for $\text{C}_{24}\text{H}_{21}\text{FN}_3\text{O}_3\text{S}$ ($M^+ + H$), 450.1283; found, 450.1282.

***N*-[4-[4-(3-Methoxyphenoxy)-2,6-dimethylphenyl]thiazol-2-yl]isonicotinamide (33)**. Yield: 51%. ^1H NMR (CDCl_3) δ 8.74 (d, $J = 6.0$ Hz, 2H), 7.62 (d, $J = 6.0$ Hz, 2H), 7.23–7.26 (m, 1H), 6.82 (s, 1H), 6.67–6.69 (m, 1H), 6.51–6.56 (m, 2H), 6.47 (s, 2H), 3.81 (s, 3H), 1.94 (s, 6H); ^{13}C NMR (CDCl_3) δ 163.71, 160.93, 158.96, 157.69, 156.65, 150.41, 147.71, 138.73, 130.15, 128.47, 120.98, 117.37, 116.70, 112.41, 111.38, 108.95, 105.45, 55.40, 20.43; ESI-MS: m/z 431.6 ($M + H$) $^+$.

***N*-[4-[4-(Benzo[d][1,3]dioxol-5-yloxy)-2,6-dimethylphenyl]thiazol-2-yl]isonicotinamide (34)**. Yield: 92%. ^1H NMR (CDCl_3) δ 8.73 (d, $J = 5.8$ Hz, 2H), 7.62 (d, $J = 5.8$ Hz, 2H), 6.81 (s, 1H), 6.78 (d, $J = 8.5$ Hz, 1H), 6.43–6.52 (m, 4H), 6.00 (s, 2H), 1.93 (s, 6H); ^{13}C NMR (CDCl_3) δ 163.38, 158.45, 157.80, 150.79, 150.57, 148.35, 147.89, 143.91, 138.82, 138.73, 128.14, 120.88, 116.39, 112.36, 112.23, 108.28, 102.32, 101.54, 20.47; ESI-MS: m/z 445.9 ($M + H$) $^+$.

Cell Proliferation Assay. The antiproliferative activity of the compounds with respect to HeLa, K562, MDA-MB-468, and MDA-MB-231 was measured using the CellTiter96 assay kit (Promega) following the manufacturer's instruction. In brief, the cells were maintained in normal glucose (1 $\mu\text{g/L}$) DMEM (Sigma, D5523) containing 10% FBS and incubated at 37 $^\circ\text{C}$ in a 5% CO_2 atmosphere. Cells were plated at a density of 2500 cells/well in a 96-well plate for 24 h, treated with different concentrations of the compounds, and incubated for another 96 h. At the end of the incubation, CellTiter 96 Aqueous One Solution Reagent (Promega) was added, and plates were

incubated for another 3 h. Cell viability was determined by measuring absorbance at 490 nm using an EMax microplate reader (Molecular Devices). Data were processed and analyzed using GraphPad Prism, version 4.

Pharmacokinetics in Rat. The pharmacokinetic properties of compounds **9a**, **12**, **17**, **31**, and **32** were determined in male Sprague–Dawley rats ($n = 3$). All procedures involving animals were performed according to protocols approved by the IACUC in the Development Center for Biotechnology. Compounds were formulated in an aqueous solution containing 5% DMSO and 10% Cremophor for IV dosing at 2.0 mg/kg and in an aqueous 1% methylcellulose solution for PO dosing at 20 mg/kg. After dosing, blood samples were taken at regular time intervals over a period of 24 h from a preimplanted catheter, and plasma was separated by centrifugation at 4000 rpm at 4 $^\circ\text{C}$. Plasma was subjected to deproteination by acetonitrile treatment, and the concentration of the compounds was determined by LC–MS/MS. Pharmacokinetic parameters were calculated using noncompartmental analysis methods in WinNonlin software (version 5.2.1, Pharsight, CA, USA).

In Vivo Xenografts. MDA-MB-231 (1×10^7 cells in matrigel/mouse) tumor cells were subcutaneously injected into the right flank of 5–8 week old female BALB/c nude (nu/nu) mice (BioLASCO, Taiwan). Tumor volume was measured with a digital caliper once tumor was palpable (within 10 to 15 days after implantation). The tumor-bearing animals were treated when the size of the tumor reached an average volume of ~ 100 mm 3 . Fifteen mice were divided into three groups and treated IV with compound **32** (20 mg/kg) or vehicle control (5% DMSO and 10% Cremophor in H_2O) at one dose per day or PO with **32** (150 mg/kg) at two doses per day for 28 days. Test compound **32** was formulated in a solution of 5% DMSO and 10% Cremophor in H_2O . The size of tumor was measured by a digital caliper and body weights of the mice were measured every 2 days. The tumor size plotted in Figure 2 represents the average tumor volume \pm SE in cubic millimeters from five mice.

Coimmunoprecipitation Analysis. K562 cells (2.5×10^6) were seeded in a 100 mm dish under serum-free conditions. After 24 h, the culture medium was changed to DMEM medium containing 10% FBS. At the same time, cells were treated with DMSO, **32**, **32** with MG132, or MG132 for 16 h. At harvest, the medium was removed, and cells were washed with ice-cold PBS. Cells were resuspended in ice-cold Lysis 250 buffer (50 mM Tris-HCl, pH 7.4, 250 mM NaCl, 5 mM EDTA, 0.1% Triton X-100, 10 mM NaF, 1 mM phenylmethylsulfonyl fluoride, and protease inhibitor cocktail (Sigma, P8340)) on ice for 30 min and then centrifuged at 12 000 rpm for 20 min at 4 $^\circ\text{C}$. The supernatants were collected for protein quantification and used for coimmunoprecipitation. Briefly, 1.3 mg of total protein from each sample was incubated with rabbit polyclonal anti-Nek2 antibody (5 μL , Rockland) or rabbit polyclonal anti-GFP antibody (5 μL , Santa cruz) as IgG control at 4 $^\circ\text{C}$. After incubation for 3 h, 100 μL of Protein A Sepharose 4 Fast Flow (50% slurry, GE healthcare) was added, and incubation continued overnight. The beads were collected, washed three times with lysis buffer, and then boiled in a SDS-loading buffer followed by SDS-PAGE. The presence of Hec1 and Nek2 were detected by western blotting with mouse monoclonal antibodies against Hec1 (GeneTex, Inc.) and Nek2 (BD Pharmingen).

Immunoblot Analysis. Cell lysates were prepared in 1 \times sample buffer (SDS sample buffer containing 62.5 mM, pH 6.8, Tris-HCl, 2% w/v SDS, 10% glycerol, 50 mM DTT, and 0.01% w/v bromophenol blue). Samples were separated by SDS-PAGE, and proteins were transferred onto PVDF membranes (GE Life Science, Piscataway, NJ, USA). The membranes were then incubated with primary antibodies in 3% bovine serum albumin in Tris-buffered saline with 0.1% Tween 20 (BSA-TBST). After washing in TBST, horseradish peroxidase-conjugated secondary antibodies were used as a tracer, and the protein signal was detected by enhanced chemiluminescence (Millipore, Billerica, MA, USA). The following primary antibodies were used for western blotting: cleaved caspase-3 (rabbit polyclonal, Cell Signaling Technology), PARP (rabbit polyclonal, Cell Signaling Technology), Mcl-1 (mouse monoclonal, BD Pharmingen), XIAP (rabbit polyclonal, Cell Signaling Technology), Bcl-2 (mouse monoclonal, Santa Cruz

Biotechnology, Inc.), Nek2 (mouse monoclonal, BD Pharmingen), Hec1 (rabbit polyclonal, GeneTex, Inc.), and actin (mouse monoclonal, Millipore).

Immunofluorescent Staining, Microscopy, and Quantification of Mitotic Abnormalities.²⁸ For immunofluorescent staining, cells were grown on Lab-Tek II Chamber Slide and washed with PBS buffer (pH 7.4) before fixation with 4% paraformaldehyde. Following permeabilization with 0.3% Triton X-100, cells were blocked with 5% BSA/PBST and incubated with anti- α -tubulin antibodies. Then, DAPI (4',6'-diamidino-2-phenylindole) staining was applied, and cells were mounted with ProLong Gold antifade (Invitrogen). Images were examined with a NIKON 80i microscope at 400 \times or 1000 \times magnification and captured with a Spot Digital Camera and Spot Advanced Software Package (Diagnostic Instruments). The percentage of cells with mitotic abnormalities was calculated by counting the number of the cells showing the abnormal mitotic figures (including chromosomal misalignment and formation of multipolar spindles) over the total number of mitotic cells counted. A minimum of 500 cells from randomly selected fields were scored per condition per experiment.

■ ASSOCIATED CONTENT

● Supporting Information

Protocols for the kinase, [³H]astemizole competitive binding, solubility, and metabolic stability assays for compound **32**. This material is available free of charge via the Internet at <http://pubs.acs.org>.

■ AUTHOR INFORMATION

Corresponding Author

*Tel.: +886 5 271 7959. Fax: +886 5 271 7901. E-mail: lukehuang@mail.ncyu.edu.tw and lukehuang0226@gmail.com.

Notes

The authors declare no competing financial interest.

■ ACKNOWLEDGMENTS

We thank Drs. Wen-Hwa Lee, Phang-Lang Chen, and Yumay Chen for their encouragement to initiate the project. We thank Drs. Chia-Lin Jeff Wang, Meng-Hsin Chen, Henry Feng, Horace H. Loh, Jui-Lien Huang, and Chi-feng Chang and Mrs. Lihyan Lee for their great leadership and support on the project. We are grateful to the Ministry of Economic Affairs of the Republic of China, Taivex Therapeutics Corporation, and the Ministry of Science and Technology of the Republic of China (102-2113-M-415-005-MY2) for financial support.

■ DEDICATION

In memory of Dr. Paonien Chen.

■ ABBREVIATIONS USED

Co-IP, coimmunoprecipitation; Hec1, highly expressed in cancer 1; Nek2, never in mitosis gene a (NIMA)-related kinase 2; *t*-BuXPhos, 2-di-*tert*-butylphosphino-2',4',6'-triisopropylbiphenyl; IV, intravenous; PBS, phosphate buffered saline; PO, per os; TBABr₃, tetrabutylammonium tribromide; hERG, human ether-a-go-go-related gene; CML, chronic myelogenous leukemia

■ REFERENCES

(1) For the biological functions of Hec1, see (a) Varma, D.; Chandrasekaran, S.; Sundin, L. J. R.; Reidy, K. T.; Wan, X.; Chasse, D. A. D.; Nevis, K. R.; DeLuca, J. G.; Salmon, E. D.; Cook, J. G. Recruitment of the human Cdt1 replication licensing protein by the loop domain of Hec1 is required for stable kinetochore–microtubule attachment. *Nat. Cell Biol.* **2012**, *14*, 593–604. (b) Wei, R. R.; Al-

Bassam, J.; Harrison, S. C. The Ndc80/HEC1 complex is a contact point for kinetochore–microtubule attachment. *Nat. Struct. Mol. Biol.* **2007**, *14*, 54–59. (c) DeLuca, J. G.; Gall, W. E.; Ciferri, C.; Cimini, D.; Musacchio, A.; Salmon, E. D. Kinetochore microtubule dynamics and attachment stability are regulated by Hec1. *Cell* **2006**, *127*, 969–982. (d) DeLuca, J. G.; Dong, Y.; Hergert, P.; Strauss, J.; Hickey, J. M.; Salmon, E. D.; McEwen, B. F. Hec1 and Nuf2 are core components of the kinetochore outer plate essential for organizing microtubule attachment sites. *Mol. Biol. Cell* **2005**, *16*, 519–531. (e) Wei, R. R.; Sorger, P. K.; Harrison, S. C. Molecular organization of the Ndc80 complex, an essential kinetochore component. *Proc. Natl. Acad. Sci. U.S.A.* **2005**, *102*, 5363–5367. (f) McClelland, M. L.; Gardner, R. D.; Kallio, M. J.; Daum, J. R.; Gorbsky, G. J.; Burke, D. J.; Stukenberg, P. T. The highly conserved Ndc80 complex is required for kinetochore assembly, chromosome congression, and spindle checkpoint activity. *Genes Dev.* **2003**, *17*, 101–114. (g) Hori, T.; Haraguchi, T.; Hiraoka, Y.; Kimura, H.; Fukagawa, T. Dynamic behavior of Nuf2–Hec1 complex that localizes to the centrosome and centromere and is essential for mitotic progression in vertebrate cells. *J. Cell Sci.* **2003**, *116*, 3347–3362. (h) Martin-Lluesma, S.; Stucke, V. M.; Nigg, E. A. Role of Hec1 in spindle checkpoint signaling and kinetochore recruitment of Mad1/Mad2. *Science* **2002**, *297*, 2267–2270.

(2) Cheeseman, I. M.; Chappie, J. S.; Wilson-Kubalek, E. M.; Desai, A. The conserved KMN network constitutes the core microtubule-binding site of the kinetochore. *Cell* **2006**, *127*, 983–997.

(3) Ciferri, C.; Musacchio, A.; Petrovic, A. The Ndc80 complex: Hub of kinetochore activity. *FEBS Lett.* **2007**, *581*, 2862–2869.

(4) Foley, E. A.; Kapoor, T. M. Microtubule attachment and spindle assembly checkpoint signalling at the kinetochore. *Nat. Rev. Mol. Cell Biol.* **2013**, *14*, 25–37.

(5) Guimaraes, G. J.; Dong, Y.; McEwen, B. F.; Deluca, J. G. Kinetochore-microtubule attachment relies on the disordered N-terminal tail domain of Hec1. *Curr. Biol.* **2008**, *18*, 1778–1784.

(6) Miller, S. A.; Johnson, M. L.; Stukenberg, P. T. Kinetochore attachments require an interaction between unstructured tails on microtubules and Ndc80 (Hec1). *Curr. Biol.* **2008**, *18*, 1785–1791.

(7) Diaz-Rodriguez, E.; Sotillo, R.; Schwartzman, J.-M.; Benezra, R. Hec1 overexpression hyperactivates the mitotic checkpoint and induces tumor formation in vivo. *Proc. Natl. Acad. Sci. U.S.A.* **2008**, *105*, 16719–16724.

(8) Chen, Y.; Riley, D. J.; Chen, P.-L.; Lee, W.-H. HEC, a novel nuclear protein rich in leucine heptad repeats specifically involved in mitosis. *Mol. Cell. Biol.* **1997**, *17*, 6049–6056.

(9) van't Veer, L. J.; Dai, H. Y.; van de Vijver, M. J.; He, Y. D. D.; Hart, A. A. M.; Mao, M.; Peterse, H. L.; van der Kooy, K.; Marton, M. J.; Witteveen, A. T.; Schreiber, G. J.; Kerkhoven, R. M.; Roberts, C.; Linsley, P. S.; Bernards, R.; Friend, S. H. Gene expression profiling predicts clinical outcome of breast cancer. *Nature* **2002**, *415*, 530–536.

(10) Glinsky, G. V.; Berezovska, O.; Glinskii, A. B. Microarray analysis identifies a death-from-cancer signature predicting therapy failure in patients with multiple types of cancer. *J. Clin. Invest.* **2005**, *115*, 1503–1521.

(11) Mo, Q.-q.; Chen, P.-b.; Jin, X.; Chen, Q.; Tang, L.; Wang, B.-b.; Li, K.-z.; Wu, P.; Fang, Y.; Wang, S.-x.; Zhou, J.-f.; Ma, D.; Chen, G. Inhibition of Hec1 expression enhances the sensitivity of human ovarian cancer cells to paclitaxel. *Acta Pharmacol. Sin.* **2013**, *34*, 541–548.

(12) Gurzov, E. N.; Izquierdo, M. RNA interference against Hec1 inhibits tumor growth in vivo. *Gene Ther.* **2006**, *13*, 1–7.

(13) Wei, R.; Ngo, B.; Wu, G.; Lee, W.-H. Phosphorylation of the Ndc80 complex protein, HEC1, by Nek2 kinase modulates chromosome alignment and signaling of the spindle assembly checkpoint. *Mol. Biol. Cell* **2011**, *22*, 3584–3594.

(14) Chen, Y.; Riley, D. J.; Zheng, L.; Chen, P.-L.; Lee, W.-H. Phosphorylation of the mitotic regulator protein Hec1 by Nek2 kinase is essential for faithful chromosome segregation. *J. Biol. Chem.* **2002**, *277*, 49408–49416.

(15) Du, J.; Cai, X.; Yao, J.; Ding, X.; Wu, Q.; Pei, S.; Jiang, K.; Zhang, Y.; Wang, W.; Shi, Y.; Lai, Y.; Shen, J.; Teng, M.; Huang, H.;

Fei, Q.; Reddy, E. S.; Zhu, J.; Jin, C.; Yao, X. The mitotic checkpoint kinase NEK2A regulates kinetochore microtubule attachment stability. *Oncogene* **2008**, *27*, 4107–4114.

(16) Qiu, X.-L.; Li, G.; Wu, G.; Zhu, J.; Zhou, L.; Chen, P.-L.; Chamberlin, A. R.; Lee, W.-H. Synthesis and biological evaluation of a series of novel inhibitor of Nek2/Hec1 analogues. *J. Med. Chem.* **2009**, *52*, 1757–1767.

(17) Wu, G.; Qiu, X.-L.; Zhou, L.; Zhu, J.; Chamberlin, A. R.; Lau, J.; Chen, P.-L.; Lee, W.-H. Small molecule targeting the Hec1/Nek2 mitotic pathway suppresses tumor cell growth in culture and in animal. *Cancer Res.* **2008**, *68*, 8393–8399.

(18) Répichet, S.; Le Roux, C.; Roques, N.; Dubac, J. BiCl₃-catalyzed Friedel–Crafts acylation reactions: bismuth(III) oxychloride as a water insensitive and recyclable procatalyst. *Tetrahedron Lett.* **2003**, *44*, 2037–2040.

(19) Lee, L. F.; Schleppe, F. M.; Howe, R. K. Syntheses and reactions of 2-halo-5-thiazolecarboxylates. *J. Heterocycl. Chem.* **1985**, *22*, 1621–1630.

(20) Anderson, K. W.; Ikawa, T.; Tundel, R. E.; Buchwald, S. L. The selective reaction of aryl halides with KOH: synthesis of phenols, aromatic ethers, and benzofurans. *J. Am. Chem. Soc.* **2006**, *128*, 10694–10695.

(21) Hames, R. S.; Wattam, S. L.; Yamano, H.; Bacchieri, R.; Fry, A. M. APC/C-mediated destruction of the centrosomal kinase Nek2A occurs in early mitosis and depends upon a cyclin A-type D-box. *EMBO J.* **2001**, *20*, 7117–7127.

(22) Hames, R. S.; Crookes, R. E.; Straatman, K. R.; Merdes, A.; Hayes, M. J.; Faragher, A. J.; Fry, A. M. Dynamic recruitment of Nek2 kinase to the centrosome involves microtubules, PCM-1, and localized proteasomal degradation. *Mol. Biol. Cell* **2005**, *16*, 1711–1724.

(23) The radiometric assays were conducted in similar manner to that of our previously published Aurora kinase assay, see: Chiang, C.-C.; Lin, Y.-H.; Lin, S. F.; Lai, C.-L.; Liu, C.; Wei, W.-Y.; Yang, S.-c.; Wang, R.-W.; Teng, L.-W.; Chuang, S. H.; Chang, J.-M.; Yuan, T.-T.; Lee, Y.-S.; Chen, P.; Chi, W.-K.; Yang, J.-Y.; Huang, H.-J.; Liao, C.-B.; Huang, J.-J. Discovery of pyrrole-indoline-2-ones as Aurora kinase inhibitors with a different inhibition profile. *J. Med. Chem.* **2010**, *53*, 5929–5941.

(24) Zhang, J.; Yang, P. L.; Gray, N. S. Targeting cancer with small molecule kinase inhibitors. *Nat. Rev. Cancer* **2009**, *9*, 28–39.

(25) Finlayson, K.; Turnbull, L.; January, C. T.; Sjarkey, J.; Kelly, J. S. [³H]Dofetilide binding to HERG transfected membranes: a potential high throughput preclinical screen. *Eur. J. Pharmacol.* **2001**, *430*, 147–148.

(26) Chiu, P. J. S.; Marcoe, K. F.; Bounds, S. E.; Lin, C.-H.; Feng, J.-J.; Lin, A.; Cheng, F.-C.; Crumb, W. J.; Mitchell, R. Validation of a [³H]astemizole binding assay in HEK293 cells expressing HERG K⁺ channels. *J. Pharmacol. Sci.* **2004**, *95*, 311–319.

(27) Yao, X.; Anderson, D. L.; Ross, S. A.; Lang, D. G.; Desai, B. Z.; Cooper, D. C.; Wheelan, P.; McIntyre, M. S.; Bergquist, M. L.; MacKenzie, K. I.; Becherer, J. D.; Hashim, M. A. Predicting QT prolongation in humans during early drug development using hERG inhibition and an anaesthetized guinea-pig model. *Br. J. Pharmacol.* **2008**, *154*, 1446–1456.

(28) Wu, G.; Wei, R.; Cheng, E.; Ngo, B.; Lee, W.-H. Hec1 contributes to mitotic centrosomal microtubule growth for proper spindle assembly through interaction with Hice1. *Mol. Biol. Cell* **2009**, *20*, 4686–4695.